ELSEVIER

www.elsevier.nl/locate/carres

Carbohydrate Research 324 (2000) 255–267

CARBOHYDRATE RESEARCH

Extracellular polysaccharide of *Erwinia chrysanthemi* A350 and ribotyping of *Erwinia chrysanthemi* spp.

James S.S. Gray, Byung Yun Yang, Rex Montgomery *

Department of Biochemistry, College of Medicine, University of Iowa, Iowa City, IA 52242, USA

Received 7 June 1999; accepted 18 August 1999

Abstract

Erwinia chrysanthemi spp. are Gram-negative bacterial phytopathogens causing soft rots in a number of plants. The structure of the extracellular polysaccharide (EPS) produced by the *E. chrysanthemi* strain A350, which is a *lac*Z$^-$ mutant of the wild type strain 3937, pathogenic to Saintpaulia, has been determined using a combination of chemical and physical techniques including methylation analysis, low-pressure gel-filtration and anion-exchange chromatography, high-pH anion-exchange chromatography, partial acid hydrolysis, mass spectrometry and 1- and 2D NMR spectroscopy. In contrast to the structures of the EPS reported for other strains of *E. chrysanthemi*, the EPS from strain A350 contains D-GalA, together with L-Rha*p* and D-Gal*p* in a 1:4:1 ratio. Evidence is presented for the following hexasaccharide repeat unit:

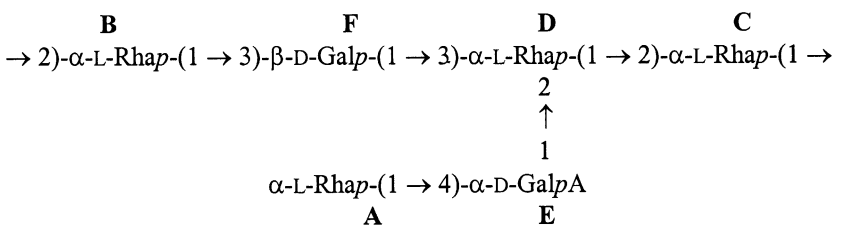

1

All the *Erwinia chrysanthemi* spp. studied to date have been analyzed by ribotyping and collated into families, which are consistent with the related structures of their EPS.

Keywords: *Erwinia chrysanthemi*; Saintpaulia; Extracellular polysaccharide; Structure; Ribotyping

1. Introduction

Erwinia chrysanthemi spp. are Gram-negative bacterial phytopathogens that cause soft rot in a number of plants [1–6]. Many of the *E. chrysanthemi* spp. produce copious amounts of extracellular polysaccharide (EPS), the role of which in host specificity and virulence is not well known. Also, little is known about the structures of the EPSs produced by strains of *E. chrysanthemi* other than

Abbreviations: COSY, correlation spectroscopy; DHB, 2,5-dihydroxybenzoic acid; GLC, gas–liquid chromatography with FID detector; GLC–MS, gas–liquid chromatography with mass-selective detector; HPAEC-PAD, high-pH anion-exchange chromatography with pulsed amperometric detection; MALDI-TOFMS, matrix-assisted laser desorption/ionization time-of-flight mass spectrometry; MALDI-TOFMS-PSD, matrix-assisted laser desorption/ionization time-of-flight mass spectrometry post-source decay; nOe, nuclear Overhauser effect; NOESY, nuclear Overhauser enhancement spectroscopy; Me_3Si, trimethylsilyl; TOCSY, total correlation spectroscopy.

* Corresponding author. Fax: +1-319-335-9570.

E-mail address: rex-montgomery@uiowa.edu (R. Montgomery)

0008-6215/00/$ - see front matter
PII: S0008-6215(99)00243-8

those determined for the corn pathogen, SR 260 [7,8], the philodendron pathogen, CU643 [9] and the potato pathogens, Ech6 [10], Ech1 and Ech9 [11]. The structures of the EPSs produced by *E. chrysanthemi* strains have been determined using a combination of chemical and physical techniques including methylation analysis, low-pressure gel-filtration and anion-exchange chromatography, high-pH anion-exchange chromatography, partial acid hydrolysis, mass spectrometry, and 1- and 2D NMR spectroscopy. It was hypothesized that a taxonomic analysis of *E. chrysanthemi* strains, both chemical and ribotyping, may indicate families that are characterized by common EPS structural features. For the EPSs studied to date this has proved to be the case and as part of this systematic study the structure of the EPS produced by *E. chrysanthemi* strain A350, a phytopathogen of Saintpaulia, is presented here.

2. Experimental

Production and purification of polysaccharide.—The *E. chrysanthemi* strains and their sources are presented in Table 1.

EPS was produced on a modified Scott's medium solidified with 1.5% agar (Difco Laboratories, Detroit, MI), supplemented with 1.5% glucose, and isolated as described previously [7,10]. The crude EPS was dialyzed against three changes of distilled water and lyophilized. The yield of the EPS was about 450 mg L^{-1} of medium.

Crude A350 EPS (2 mg mL^{-1} in phosphate-buffered saline, PBS, pH 7.3) was purified by fractional precipitation with acetone followed by low-pressure gel-permeation and anion-exchange chromatographies. Gel-filtration was performed on a ToyoPearl HW65F column (1.5×100 cm, TosoHaas, Montgomeryville, PA), eluting with 1% NaCl, where the EPS eluted as a broad peak with a molecular weight > 66 KDa, using a dextran standard. Fractions were pooled appropriately and chromatographed on a ToyoPearl DEAE-650M (TosoHaas, Montgomeryville, PA) anion-exchange column (1.5×15 cm) that had been equilibrated in water and eluted with a linear gradient of 0–500 mM KCl. The EPS eluted as a single peak at about 210 mM KCl. The fractions containing EPS were pooled, electrodialyzed and lyophilized for further analysis.

Analytical and general methods.—The methods used for methylation analysis, GLC and GLC–MS, uronic acid reduction by Super-Deuteride after methylation, determination of the absolute configuration of the monosaccharides, monosaccharide analysis by HPAEC-PAD and by GLC have been described elsewhere [7,10,12].

Table 1
E. chrysanthemi strains used in this study and their origin

Strain	Host	Source	Notes
SR31	Corn	A. Kelman, University of Wisconsin, Madison, USA	EC16
SR260	Corn	J. Mildenhall, University of Fort Hare, Alice, South Africa	Isolated from University of Fort Hare Farm, Alice, South Africa
Ech1	Potato	C.N. Marasas, Vegetable and Ornamental Plant Institute, Pretoria, South Africa	*Erwinia* wilt (Douglas, South Africa)
Ech6	Potato	C.N. Marasas, Vegetable and Ornamental Plant Institute, Pretoria, South Africa	*Erwinia* wilt (Highveld, South Africa)
Ech9	Potato	C.N. Marasas, Vegetable and Ornamental Plant Institute, Pretoria, South Africa	Black leg (Douglas, South Africa)
Ech378	Dieffenbachia	E. Braun, Iowa State University, Ames, USA	Garibaldi, Italy
CU643	Philodendron	E. Braun, Iowa State University, Ames, USA	Garibaldi, Italy
A350	Saintpaulia	G. Condemine, Laboratory of Microbial Molecular Genetics and Cellular Interactions, Lyon, France	*lac*Z^- derivative of strain 3937
A2148	Saintpaulia	G. Condemine, Laboratory of Microbial Molecular Genetics and Cellular Interactions, Lyon, France	*Pec*T, elevated EPS production

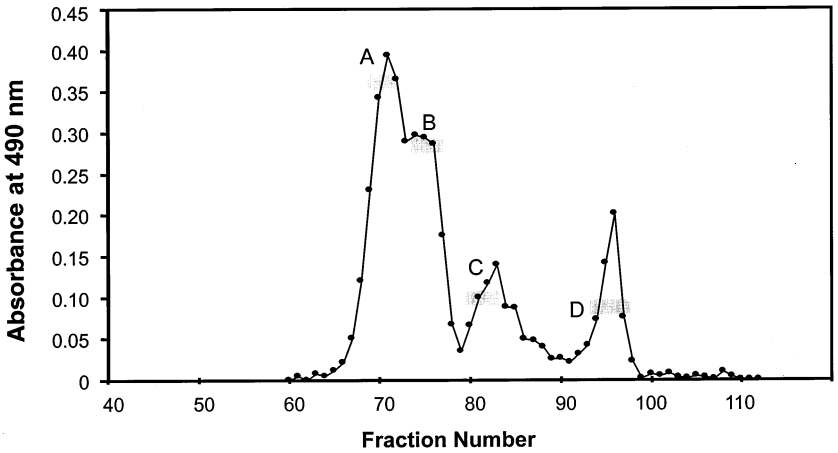

Fig. 1. Chromatography of oligosaccharides produced by fuming HCl treatment of A350 EPS on Bio-Gel P-4 (1.5 × 86 cm) and eluted with 100 mM NH_4OAc. Fractions were pooled as indicated by the bars (fractions A to D) and purified by HPAEC.

Partial hydrolysis of EPS by fuming HCl.—Partial acid hydrolysis with fuming HCl was performed as described previously [12,13]. Briefly, an electrodialyzed sample of A350 EPS (25 mg) was dissolved in 4.5 mL of fuming HCl (37.5%, sp. gr. ≈ 1.19, Fisher Scientific, Pittsburgh, PA) with vigorous stirring and intermittent cooling on ice, warmed to 40 °C and held at this temperature for 30 min. The solution was cooled on ice, neutralized with 0.5 M NaOH (pH paper), and lyophilized.

The lyophilized sample was dissolved in water (10 mL), any precipitate removed by centrifugation and then desalted on a Bio-Gel P-2 column (2.5 × 18 cm, −400 mesh), eluting with water. The oligosaccharide fractions were pooled appropriately, lyophilized, dissolved in water (2 mL) and further purified by chromatography on a Bio-Gel P-4 column (1.5 × 86 cm, 200–400 mesh), eluting with 100 mM NH_4OAc. Carbohydrate-containing fractions were analyzed by MALDI-TOFMS, pooled according to their molecular weights (Fig. 1) and recovered by lyophilization.

HPAEC purification of acid oligosaccharides.—Each of the pooled fractions from the Bio-Gel P-4 column was further purified by HPAEC on a CarboPac PA1 column (4.0 × 250 mm, Dionex Corporation, Sunnyvale, CA). Isocratic elution with 40 mM NaOH–60 mM NaOAc was found to be optimal for separation of the oligosaccharides. Each peak was collected manually and either neutralized immediately with glacial AcOH or reduced with a 30 molar excess of $NaBH_4$ for 2 h. After reduction, excess borohydride was quenched with AcOH and the borate was removed by repeated evaporation from 10% AcOH in MeOH and finally from MeOH. The peaks were recovered by lyophilization after removal of Na^+ on a spin column (0.5–1.0 mL) of Bio-Rad AG50W-X8, H^+.

The purity of the oligosaccharides was assessed by rechromatography on the CarboPac PA1 column eluted isocratically with either 40 or 100 mM NaOH and a 50–150 mM NaOAc gradient and by MALDI-TOFMS.

Degradation of polysaccharide by lithium in ethylenediamine.—Electrodialyzed A350 EPS (4 mg) was treated with Li in ethylenediamine and worked up as described by Lau et al. [14,15]. The degradation products were fractionated by chromatography on a Bio-Gel P-2 column (1.0 × 45 cm, 200–400 mesh; Bio-Rad Laboratories, Hercules, CA), eluting with water. The fraction eluting in the void volume of the column was lyophilized.

The low-molecular-weight fraction was analyzed by GLC of the acetylated products.

Matrix-assisted laser desorption/ionization-time-of-flight mass spectrometry (MALDI-TOFMS) and matrix-assisted laser desorption/ionization time-of-flight mass spectrometry post-source decay analyses (MALDI-TOFMS-PSD).—MALDI-TOFMS was performed on a Voyager-DE STR BioSpectrometry Workstation (PerSeptive Biosystems, Framingham,

MA) operating in the positive-ion mode with an accelerating voltage of 25 kV. 2,5-Dihydroxybenzoic acid (2 μL) (DHB) (10 mg mL^{-1} in 10% aq EtOH) and 1 μL of oligosaccharide in water or per-*O*-methylated oligosaccharide dissolved in EtOH (10–100 pmol) were sequentially loaded onto the target plate, allowed to air-dry and recrystallized from 0.5 mL abs EtOH. Maltoheptaose (Boehringer Mannheim, NY), or its per-*O*-methylated derivative, was used as an external standard.

Post-source decay (PSD) sequencing of the per-*O*-methylated oligosaccharides was performed on a Voyager-DE STR BioSpectrometry Workstation with an accelerating voltage of 25 kV, a grid voltage of 75% and a guidewire voltage of 0.020 to 0.000% depending upon the mirror ratio. All analyses were performed with DHB as a matrix.

NMR analyses.—^{1}H NMR 1- and 2D analyses were acquired on a Bruker AMX-600 NMR spectrometer (^{1}H at 600.13 MHz; ^{13}C at 150.92 MHz). Proton spectra were acquired with a 5 mm proton-only probe using standard Bruker software as described previously [7,9]. NOESY spectra of both the native EPS and the EPS backbone were obtained with a 150 ms mixing time. TOCSY spectra were acquired with a 120 ms (native EPS) or a 150 ms (EPS backbone) mixing time. HMQC and HMBC spectra were acquired with a 5 mm broadband inverse probe with delays of 3.333 and 60 ms, respectively (decoupling optimized for $\sim$150 and $\sim$8 Hz, respectively). A HMQC spectrum of the native EPS without decoupling was acquired to measure the H-1/C-1 ($^1J_{\text{H-1–C-1}}$) coupling constants.

All data were processed on a Silicon Graphics O2 (Mountain View, CA) with Felix 95.0 (Biosym Technologies, San Diego, CA).

Biochemical studies and ribotyping.—Each of the *E. chrysanthemi* strains in Table 1 was subjected to the API-20E and Vitek (bioMerieux sa, Lyon, France) test systems according to the kit instructions. Molecular typing was performed on a Riboprinter™ Microbial Characterization System (Qualicon, Inc., Wilmington, DE) using the manufacturers reagents and instructions. The restriction enzyme used for DNA cleavage was *Eco*R1.

3. Results and discussion

Purification and composition of EPS.—Monosaccharide analysis of fractions across the carbohydrate peak from both the gel filtration and the DEAE-650M columns revealed a similar composition. No neutral oligo- or polysaccharides were present in the A350 EPS preparations.

Only Rha, Gal and GalA were detected in acid hydrolyzates of A350 EPS by HPAEC-PAD analysis and in methanolyzates by GLC of the trimethylsilyl (Me_3Si) derivatives. GLC analysis of the Me_3Si derivatives of the (*R*)-(−)-butan-2-ol glycosides, as described by Gerwig et al. [16], revealed that Rha was of the L configuration and both Gal and GalA were of the D configuration. The composition of carboxyl-reduced EPS was found to be L-Rha and D-Gal in the ratio 4:2. The detection of 6,6′-dideuterio-galactitol hexaacetate by GLC–MS provided proof that one of the Gal residues is derived from GalA. Thus, the composition of the native EPS is L-Rha, D-Gal and D-GalA in a 4:1:1 ratio.

Degradation of A350 by lithium in ethylenediamine.—Two fragments were generated by degradation of A350 with lithium in ethylenediamine and were separated by chromatography on Bio-Gel P-2.

The high-molecular-weight backbone fragment, which eluted in the void volume of the column, contained Rha and Gal in the mol ratio 3:1.

Rha_{ol} (major) and Rha (minor) were the only sugars detected in the low-molecular fraction of the Li–ethylenediamine degradation products.

Methylation analysis of A350 EPS and the A350 EPS backbone.—Methylation analysis of native A350 EPS revealed the presence of a terminal Rha (one residue), two residues of 2-substituted Rha and one residue each of 2,3-substituted Rha and 3-substituted Gal. In addition to these residues, reduction of the methyl ester of the uronic acid in the methylated A350 EPS with Super-Deuteride (lithium triethylborodeuteride) before hydrolysis and subsequent work-up revealed the presence of 4-substituted GalA (detected as 1,4,5,6 tetra-*O*-acetyl-1,6,6′-trideuterio-2,3-di-*O*-methyl-galactitol) (Table 2).

Methylation analysis of the A350 EPS backbone (derived from Li–ethylenediamine degradation of the A350 EPS) revealed the presence of two residues of 2-substituted Rha, one residue of 3-substituted Rha and one residue of 3-substituted Gal (Table 2).

These data are consistent with a hexasaccharide repeat subunit for the A350 EPS in which a side chain, Rha-(1→4)-GalA, is attached to 2-O of a Rha residue in a tetrasaccharide backbone repeat composed of →2)-Rha-(1→(two residues), →2,3)-Rha-(1→ (one residue) and →3)-Gal-(1→ (one residue).

It is evident from the methylation analysis that all of the residues in the EPS are in the pyranose form.

Partial acid hydrolysis and purification of oligosaccharides.—Fuming HCl has been successfully used for the non-specific depolymerization of very viscous solutions of EPS [13] and for the preparation of oligosaccharides [12]. Treatment of A350 EPS for 30 min at 40 °C gave rise to a series of oligosaccharides ranging in size from the aldobiuronic acid (peak D, Fig. 1) to the aldopentauronic acid (peak A, Fig. 1). No high-molecular-weight species remained after this treatment.

The presence of only Rha, Gal, and GalA in the EPS allowed unique monosaccharide compositions to be determined for the oligosaccharides by MALDI-TOFMS analysis of the per-*O*-methylated derivatives. Peak A was identified as a pentasaccharide composed of three Rha residues and one residue each of GalA and Gal [*m*/*z* (obs.) 1013.2, *m*/*z* (calc.) 1013.7). Peaks B, C, and D (Fig. 1) were identified as the tetrasaccharide [GalA(Rha)$_3$, *m*/*z* 809.3 (obs.), 809.5 (calc.)], trisaccharide [GalA(Rha)$_2$, *m*/*z* 635.2 (obs.), 635.4 (calc.)], and the disaccharide [GalA(Rha), *m*/*z* 461.4 (obs.), 461.5 (calc.)], respectively. These monosaccharide compositions were confirmed by HPAEC-PAD analyses after acid hydrolysis of the oligosaccharides. Each of these oligosaccharide fractions was further purified by HPAEC (Fig. 2).

Sequencing of oligosaccharides A to D.—The sequence of each of the purified oligosaccharides A to D was principally established from methylation linkage analysis and mass spectrometry. After methylation, a small portion of the per-*O*-methylated oligosaccharide was set aside for sequencing by MALDI-TOFMS-PSD analysis. Super-Deuteride was used to reduce the methyl ester of the uronic acid in the rest of the sample, which was subsequently hydrolyzed, reduced with sodium borodeuteride, acetylated and analyzed by GLC and GLC–MS.

The presence of 1,5,6-tri-*O*-acetyl-2,3,4-tri-*O*-methyl-1,6,6′-trideuterio-galactitol and 2-*O*-acetyl-1,3,4,5-tetra-*O*-methyl-rhamnitol in a ratio of 1:1 provided an unambiguous sequence for the aldobiuronic acid, GalA-(1→2)-Rha. The sequences of the aldotriuronic [GalA-(1→2)-Rha-(1→2)-Rha, oligosaccharide C] and the aldotetrauronic acid [GalA-(1→2)-Rha-(1→2)-Rha-(1→2)-Rha, oligosaccharide B] were also unambiguously defined by methylation analysis with the generation of 1,5,6-tri-*O*-acetyl-2,3,4-tri-*O*-methyl-1,6,6′-trideuterio-galactitol, 1,2,5-tri-*O*-acetyl-3,4-di-*O*-methyl-rhamnitol and 2-*O*-acetyl-1,3,4,5-tetra-*O*-methyl-rhamnitol in ratios 1:1:1 and 1:2:1, respectively. The sequence of pentasaccharide A, GalA-(1→2)-Rha-(1→2)-Rha-(1→2)-Rha-(1→3)-Gal, also followed directly from the methylation analysis, where 1,5,6-tri-*O*-acetyl-1,6,6′-trideuterio-2,3,4-tri-*O*-methyl galactitol, 1,2,5-tri-*O*-acetyl-3,4-di-*O*-methyl-rhamnitol and 3-*O*-acetyl-1,2,4,5,6-penta-*O*-methyl-galactitol in the ratio 1:3:1 were observed.

Table 2
Methylation analyses of *E. chrysanthemi* A350 EPS and A350 EPS backbone derived from Li–ethylenediamine treatment

Sugar [a]	Mol ratio	
	EPS **1**	EPS backbone **2**
2,3,4-*O*-Me$_3$Rha	1.0	
3,4-*O*-Me$_2$Rha	1.8	1.9
2,4-*O*-Me$_2$Rha		0.8
4-*O*-MeRha	1.2	
2,4,6-*O*-Me$_3$Gal	1.0	1.0
2,3,-*O*-Me$_2$GalA [b]	1.0	

[a] 2,3,4-*O*-Me$_3$Rha = 1,5-di-*O*-acetyl-1-deuterio-2,3,4-tri-*O*-methyl rhamnitol, etc.

[b] Observed as 1,4,5,6-tetra-*O*-acetyl-1,6,6′-trideuterio-2,3-di-*O*-methyl galactitol derived from the reduction of the methyl ester of 2,3-Me$_2$GalA with Super-Deuteride.

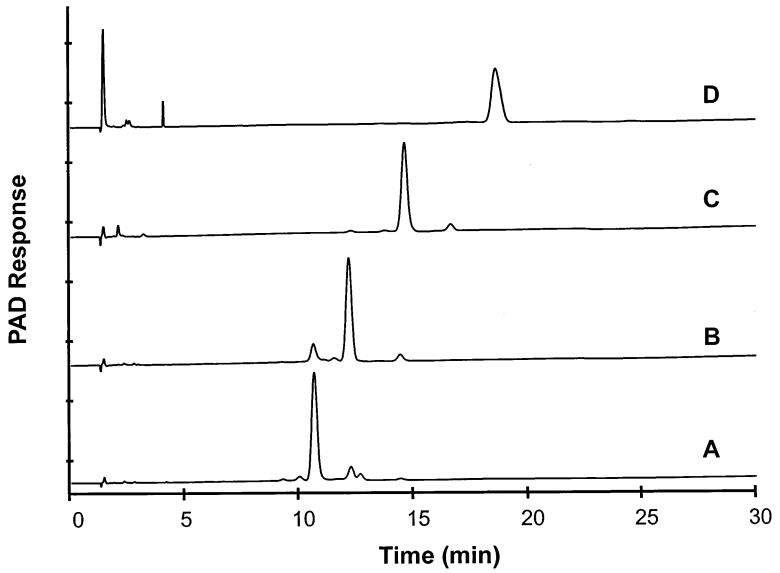

Fig. 2. Purification of fractions A to D from Bio-Gel P-4 chromatography by HPAEC on a CarboPac PA1 column (4.0 × 250 mm) eluted isocratically with 40 mM NaOH–60 mM NaOAc. The peaks were collected manually and either neutralized immediately with HOAc or reduced with $NaBH_4$.

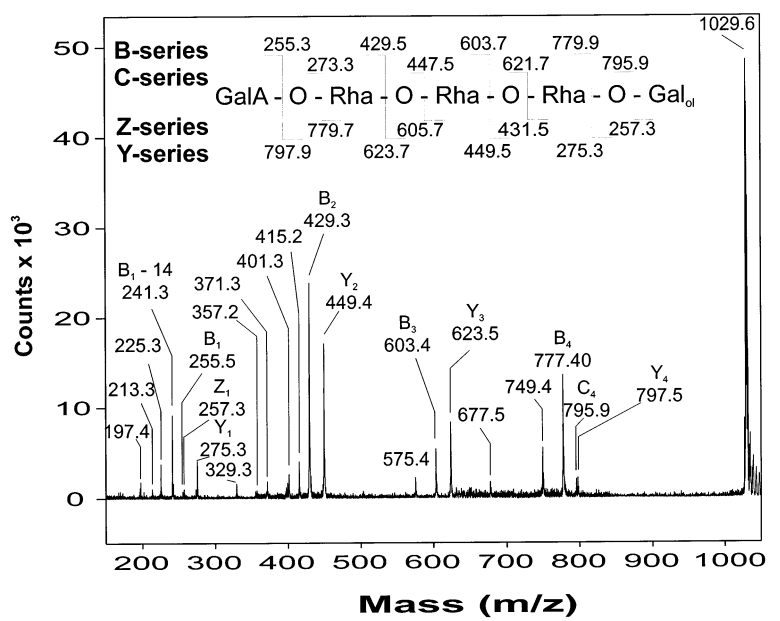

Fig. 3. MALDI-TOFMS-PSD sequencing of pentasaccharide A.

The sequence of the aldotetrauronic acid (oligosaccharide B) and the aldopentauronic acid (oligosaccharide A) were also determined by MALDI-TOFMS-PSD (illustrated for the pentamer in Fig. 3), where a series of B-, C-, Y- and Z-ions (nomenclature of Domon and Costello [17]) were observed with the B- and Y-ions dominating. These analyses confirm the sequences determined by methylation analysis.

All of these data are consistent with structure **1** proposed for the A350 EPS.

1D ^1H NMR analyses of A350 EPS and backbone.—The study of the sequences of the oligosaccharides and the methylation data gave strong evidence for the sequence **1**. Confirmation was obtained by ^1H NMR analysis of A350 EPS (in the presence and absence of 1% NaCl) and the linear backbone that resulted from treatment of the EPS with lithium in ethylenediamine.

The 1D ^{1}H NMR spectrum of the native EPS obtained in D_2O is characterized by broad lines (Fig. 4, top spectrum). The signals become much sharper when the spectrum is acquired in the presence of 1% NaCl (Fig. 4, middle spectrum) and individual coupling can now be observed for most of the signals. Inspection of the spectrum acquired in 1% NaCl shows seven signals downfield of the HOD peak: δ 5.252 ppm ($J_{1,2}$ 1.2 Hz, 1 H), δ 5.141 ppm ($J_{1,2}$ unresolved, 2 H), δ 5.082 ppm ($J_{1,2}$ unresolved, 1 H), δ 5.064 ppm ($J_{1,2}$ 3.6 Hz, 1 H), δ 4.676 ppm ($J_{1,2}$ 1.2 Hz, 1 H), δ 4.645 ppm ($J_{1,2}$ 7.2 Hz, 1 H), δ 4.447 ppm ($J_{1,2}$ unresolved, 1 H). The signals at δ 4.645 and 5.064 ppm are characteristic of the β- and α-*gluco* or *galacto* configuration and therefore arise from the Gal and GalA. The signals at δ 4.447 and 4.676 ppm are non-anomeric (see below) and typical of H-5 and H-4 of 4-linked α-GalA residues [18–21], thus suggesting that the anomeric resonance at δ 5.064 arises from an α-linked GalA residue. This is indeed the case as shown below. The remaining anomeric signals at δ 5.252, 5.141 and 5.082 ppm arise from the Rha residues. Twelve protons (four doublets, $J_{1,2}$ 6.0 Hz), corresponding to the four 6-deoxy groups of Rha, are observed at δ 1.247, 1.285, 1.295, and 1.305 ppm.

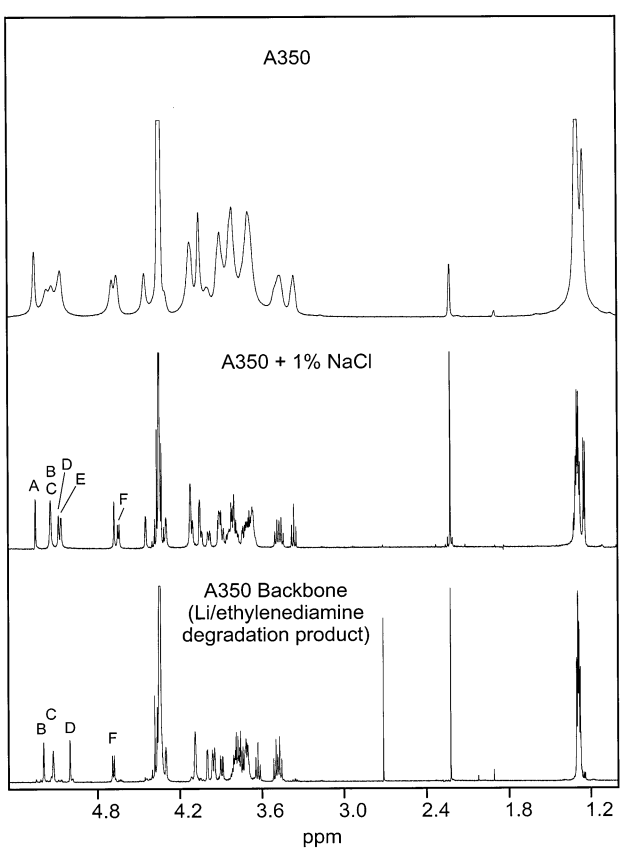

Fig. 4. 1D NMR spectra acquired at 338 K and 600.14 MHz of native A350 EPS in D_2O (top panel), native A350 EPS in 1% NaCl in D_2O (middle panel) and A350 EPS backbone in D_2O (bottom panel). The anomeric protons are labeled A to F from low to high field (high δ_H to low δ_H).

The 1D NMR spectrum of the A350 EPS backbone is much simpler, showing four anomeric resonances at δ 5.196 ppm ($J_{1,2}$ unresolved, 1 H), δ 5.126 ($J_{1,2}$ unresolved, 1 H), δ 5.004 ($J_{1,2}$ unresolved, 1 H) and δ 4.687 ($J_{1,2}$ 7.5 Hz, 1 H) corresponding to three Rha residues and one Gal residue, respectively (Fig. 4, bottom spectrum). Three doublets, δ 1.278, 1.293 and 1.301 ppm ($J_{1,2}$ 6.0 Hz), arising from the three 6-deoxy groups of the Rha residues are also present. These data are consistent with the presence of a tetrameric repeat unit in the A350 backbone.

No pyruvate or acetate was detected in the A350 EPS by ^{1}H NMR spectroscopy.

2D ^{1}H NMR analyses of A350 EPS and A350 backbone.—A combination of COSY, TOCSY, HMQC and HMBC experiments was utilized to assign completely the ^{1}H and ^{13}C resonances of the A350 backbone (Table 3) and the ^{1}H resonances of the A350 EPS (Table 4).

A350 backbone. The anomeric signals were labeled B, C, D and F from low to high field i.e., decreasing δ (Fig. 4, bottom spectrum). These labels were chosen to be consistent with the labeling of the A350 EPS spectrum (Fig. 4, middle spectrum).

The H-1, H-2, H-3, and H-4 resonances for Rha-B, Rha-C, and Rha-D were completely assigned in the COSY spectrum, using the TOCSY spectrum to resolve any ambiguities (Table 3). The H-5 resonances of these residues were not readily observed in the 1D spectrum because of their complexity and these chemical shifts were extracted from the clearly defined cross-peaks between H-6 and H-5 and H-4 and H-5 of these residues in the COSY spectrum.

The chemical shifts of H-1 to H-4 of Gal-F were obtained directly from the COSY and TOCSY spectra. The chemical shift of the equatorial H-4 is clearly visible downfield of

Table 3
Chemical shifts for the sugar residues in the *E. chrysanthemi* A350 backbone produced by Li–ethylenediamine degradation of A350 EPS [a]

→2)-α-L-Rha*p*-(1→3)-β-D-Gal*p*-(1→3)-α-L-Rha*p*-(1→2)-α-L-Rha*p*-(1→
B F D C

Residue	δ_H (ppm) [b]/$^3J_{H/H}$ (Hz)/δ_C (ppm) [c]						
	1	**2**	**3**	**4**	**5**	**6a**	**6b**
→2)-α-L-Rha-(1→ B	5.196 (<1.0) 101.5	4.090 (2.9) 78.7	3.956 (9.8) 71.1	3.501 (9.6) 73.2	3.807 (6.0) 69.9	1.301 17.5	
→2)-α-L-Rha-(1→ C	5.126 (<1.0) 101.6	4.090 (3.2) 78.7	3.897 (9.7) 70.9	3.483 (9.6) 73.3	3.722 (6.0) 71.9	1.278 17.5	
→3)-α-L-Rha-(1→ D	5.004 (<1.0) 102.6	4.304 (2.9) 70.8	3.956 (9.8) 80.8	3.632 (9.6) 72.1	3.79 (~6.0) 70.0	1.293 17.5	
→3)-β-L-Gal-(1→ F	4.687 (7.5) 104.8	3.758 (10.2) 72.0	3.73 (2.7) 80.3	3.985 (<1) 69.3	~3.70 75.8	3.79 61.7	3.75

[a] The chemical shifts were assigned by a combination of 1- and 2D NMR experiments as described in the text.
[b] Chemical shifts relative to acetone (δ_H 2.225 ppm; δ_C 31.07 ppm).
[c] Proton chemical shifts derived from 1D spectrum reported to three decimal places (error ± 0.002 ppm); those from 2D spectra reported to two decimal places (error ± 0.01 ppm). Carbon chemical shifts extracted from the HMQC spectrum (error ± 0.1 ppm).

H-1, H-2, and H-3 (δ 3.985, $J_{3,4}$ 2.7 Hz and $J_{4,5} \sim 1$ Hz). The assignment of H-5, H-6a, and H-6b of Gal-F was more difficult because of their closeness. The small coupling constant between Gal-F H-4 and H-5 also reduced the intensity of the H-5, H-6a, and H-6b cross-peaks in the H-1 track of the TOCSY spectrum. Nonetheless, the chemical shift for H-5 could be assigned from the weak cross-peak between H-4 and H-5, which appears slightly up-field of the H-3/H-4 cross-peak. Both H-6a and H-6b were identified with some difficulty in the COSY spectrum as cross-peaks close to the diagonal (δ 3.79 and 3.75 ppm, respectively). Both assignments were confirmed from the HMQC spectrum, where two proton resonances associated with δ_C at 61.7 ppm were seen.

Insufficient backbone material was available to run a ^{13}C NMR spectrum. All of the δ_c values in Table 3 were extracted from the HMQC spectrum.

The shift downfield of δ_C for C-2 of Rha-B and Rha-C, and C-3 of Rha-D (about 7–10 ppm from that observed in non-substituted Rha residues [22,23]) confirms their involvement in glycosidic linkages. Similarly the downfield shift of δ_C for H-3 of Gal-F corroborates its involvement in a glycosidic linkage [23].

The β-linkage of Gal-F is clear from the upfield position of H-1 (δ 4.687) and its coupling constant ($J_{1,2}$ 7.5 Hz). This assignment is also supported by the intra-residue nOes between H-1 and H-3 and H-5 of Gal-F. Further support for this assignment comes from the $J_{H\text{-}1\text{–}C\text{-}1}$ value of 160 Hz, characteristic for β-linkages [24], obtained from the one bond coupling pattern observed in the HMBC spectrum.

The assignment of α-linkages to three Rha residues is supported by two lines of evidence. Firstly, the downfield shift of the chemical shifts for the H-5 protons of these residues (δ 3.72–3.81 ppm) is typical of α-linked residues [22,25,26]. Secondly, the $J_{H\text{-}1\text{–}C\text{-}1}$ values of 170–175 Hz extracted from the one-bond coupling observed in the HMBC spectrum are characteristic of α linkages [24].

The sugar sequence of the EPS backbone is readily extracted from the 2D NOESY spectrum (Fig. 5). The nOes between H-1 of Rha-B and H-3 of Gal-F, H-1 of Rha-C and H-2 of Rha-B, H-1 of Rha-D and H-2 of Rha-C, and H-1 of Gal-F and H-3 of Rha-D provide proof of the following sequence for the EPS backbone:

$$\rightarrow 2)\text{-}\alpha\text{-L-}\underset{\mathbf{B}}{\text{Rha}}\text{-}(1\rightarrow 3)\text{-}\beta\text{-D-}\underset{\mathbf{F}}{\text{Gal}}\text{-}(1\rightarrow 3)\text{-}$$
$$\alpha\text{-L-}\underset{\mathbf{D}}{\text{Rha}}\text{-}(1\rightarrow 2)\text{-}\alpha\text{-L-}\underset{\mathbf{C}}{\text{Rha}}\text{-}(1\rightarrow$$

Other nOes are also observed in Fig. 5; these are mainly due to intra-residue interactions viz., B1/B2, C1/C2, D1/D2 and F1/F2, F1/F3 and F1/F5 (the latter are not well resolved). The weak inter-residue nOe between H-1 of Rha-C and H-5 of Rha-B is similar to interactions observed previously between adjacent (1→2)-linked Rha residues [9]. These may reflect conformational changes, either in the EPS allowing these two protons to move within 4–5 Å of each other, or changes in the ring conformation of Rha-C as has been proposed by Widmalm et al. [27].

As observed with the EPS from *E. chrysanthemi* strain CU643 [9], the HMBC experiment proved of little use in assigning the complete sequence of the A350 backbone, due mainly to the low resolution of the ^{13}C spectrum and the similarity in the carbon chemical shifts of the atoms involved in the glycosidic

Table 4
NMR data for *E. chrysanthemi* A350 EPS [a]

A **E**

α-L-Rha*p*-(1→4)-α-D-Gal*p*A
1
↓
2

→2)-α-L-Rha*p*-(1→3)-β-D-Gal*p*-(1→3)-α-L-Rha*p*-(1→2)-α-L-Rha*p*-(1→

B **F** **D** **C**

Residue	δ_H (ppm)/^3J (Hz) [b,c]						
	1	**2**	**3**	**4**	**5**	**6**	**6′**
α-L-Rha*p*-(1→ **A**	5.252 (1.2)	4.053 (3.0)	3.808 (9.6)	3.363 (10.0)	3.805 (6.0)	1.247	
→2)-α-L-Rha*p*-(1→ **B**	5.141 (<1.0)	4.121 (3.0)	3.985 (9.6)	3.486 (9.3)	3.844 (6.0)	1.295	
→2)-α-L-Rha*p*-(1→ **C**	5.141 (<1.0)	4.121 (3.0)	3.887 (9.5)	3.457 (10.5)	3.718 (6.6)	1.285	
→2,3)-α-L-Rha*p*-(1→ **D**	5.082 (<1.0)	4.297	4.045 (9.6)	3.688 (10.5)	3.784 (5.4)	1.305	
→4)-α-D-Gal*p*A-(1→ **E**	5.064 (3.6)	3.909 (9.9)	4.112 (10.5)	4.447 (<1.0)	4.676		
→3-β-D-Gal*p*-(1→ **F**	4.645 (7.2)	3.678 (10.8)	3.661 (3.9)	3.910 (<1.0)	~3.66 (3.3 [d] 4.5 [e])	3.807 (11.7 [f])	3.727

[a] The EPS was exchanged into D_2O containing 1% NaCl and COSY, TOCSY and HMQC spectra were acquired and analyzed as described in the text.

[b] Chemical shifts relative to acetone (δ_H 2.225 ppm; δ_C 31.07).

[c] Proton chemical shifts derived from 1D spectrum reported to three decimal places (error ± 0.002 ppm); those from 2D spectra reported to two decimal places (error ± 0.01 ppm).

[d] $^3J_{5,6a}$.

[e] $^3J_{5,6b}$.

[f] $^3J_{6a,6b}$.

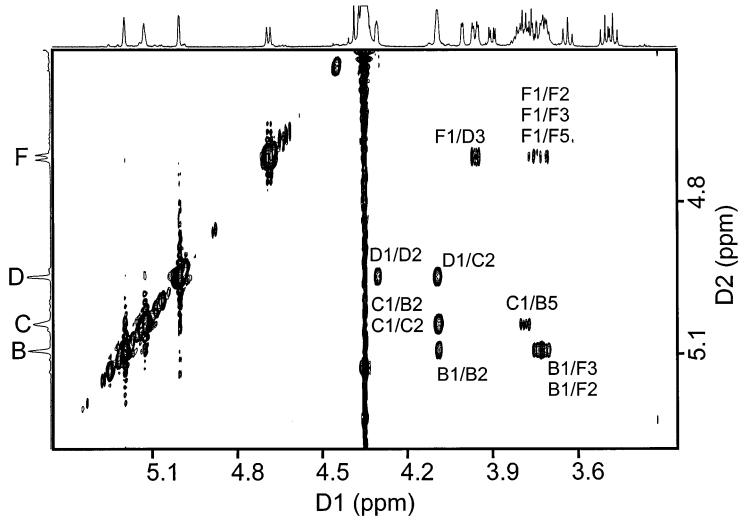

Fig. 5. 2D NOESY spectrum of A350 EPS backbone acquired at 338 K and 600.14 MHz. The mixing time was 120 ms. Both intra- and inter-residue cross-peaks are identified and labeled.

bonds. It was possible, however, to confirm that Gal-F was linked to O-3 of Rha-D (cross-peak between δ_H 3.956 ppm and δ_C 104.8 ppm). Consequently, the 2-linked Rha residues are adjacent to one another, confirming the sequence of the A350 backbone as shown above.

A350 EPS. The anomeric protons were labeled A–F with decreasing δ i.e., low to high field (Fig. 4, middle panel).

A COSY experiment performed on A350 EPS in D_2O was unsuccessful and very few cross-peaks were observed. This spectrum was not studied further, attention being concentrated on the COSY, NOESY and TOCSY spectra acquired at 338 K of the EPS in 1% NaCl in D_2O. These spectra were of sufficient quality to assign all the proton resonances in the A350 EPS (Table 4).

The signals arising from H-1, H-2, H-3 and H-4 of Rha residues A to D were readily assigned from the COSY and TOCSY spectra and their chemical shifts and coupling constants were extracted from the 1D spectrum. The signals from H-1 and H-2 of Rha residues B and C are coincident and diverge from H-3. The H-5 signals for the Rha residues could not be extracted from the 1D spectrum as explained above and the cross-peaks from H-4 and H-6 of these residues were used as entry points to obtain the chemical shifts of these protons. The entire spin system for GalA-E was observed and identified in the COSY spectrum and the signals at δ 4.447 and 4.676 were unambiguously identified as arising from H-4 and H-5, respectively. The difficulties in assigning H-4, H-5, H-6a and H-6b of Gal-F were similar to those described above for the A350 backbone and were resolved in a similar fashion. The chemical shifts and those coupling constants that could be extracted are presented in Table 4.

The sequence of the A350 EPS was obtained by analysis of the 2D NOESY spectrum (Fig. 6). A number of nOe cross-peaks viz. between Rha-A H-1 and GalA–E H-4 (δ 5.252 and 4.447 ppm), GalA–E H-1 and Rha-D H-2 (δ 5.064 and 4.297 ppm), and Gal-F H-1 and Rha-D H-3 (δ 4.645 and 4.045 ppm) are consistent with the following partial sequence:

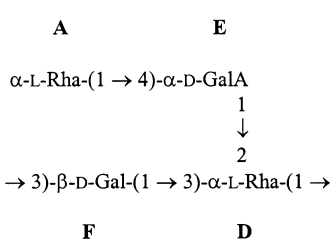

The resonances arising from H-1 of Rha-B and Rha-C are indistinguishable as are those for H-2 of Rha-B and Rha-C (Figs. 4 and 6). Consequently, the sequence of these two residues cannot be directly determined from their H-1/H-2 NOESY cross-peaks. It is evident from the NOESY spectrum in Fig. 6 that

Rha-D is linked to O-2 of either Rha-B or Rha-C (nOe between δ 5.082 and 4.121 ppm) and that either Rha-B or Rha-C is linked to O-3 of Gal-F (nOe between 5.141 and δ 3.661 ppm). The strong cross-peak between δ 5.141 and 4.121 ppm in the NOESY spectrum (Fig. 6) also suggests that this represents not only the expected intra-residue nOes (H-1/H-2) for Rha-B and Rha-C, but also an inter-residue nOe between H-1 of Rha-B and H-2 of Rha-C (or vice versa). Evidence for the correct sequence of these two residues is provided by the weak nOe between H-1 of Rha-D and H-3 of Rha-C (δ 5.082 and 3.887 ppm) (Fig. 6). This observation, together with previous reports that nOes can occur between the anomeric proton and protons adjacent to those involved in the glycosidic linkage [7,9,28], is consistent with the sequence Rha-D → Rha-C. Since this precludes the sequence, Rha-B → Rha-C, the strong NOESY cross-peak between δ 5.141 and 4.121 ppm arises from both intra-residue (Rha-B H-1/H-2 and Rha-C H-1/H-2) and inter-residue (Rha-C H-1/Rha-B H-2) interactions. It follows that the nOe between δ 5.141 and 3.661 ppm is due to the interaction between H-1 of Rha-B and H-3 of Gal-F. These data, together with the weak nOe between δ 5.141 and 3.985 ppm (assigned to an inter-residue nOe between H-1 of Rha-C and H-3 of Rha-B), support the backbone sequence Rha-B → Gal-F → Rha-D → Rha-C.

The anomeric configurations of Rha-A, B, C, and D and GalA-E are all α as evidenced from the $J_{H\text{-}1\text{–}C\text{-}1}$ values of 170 to 175 Hz extracted from a HMQC spectrum acquired without decoupling. Similarly, $J_{H\text{-}1\text{–}C\text{-}1}$ of 159 Hz for the anomeric proton of Gal-F proves that it is β linked.

All these data allow the sequence **1** to be proposed for the EPS from *E. chrysanthemi* strain A350.

Comparison of the extracellular polysaccharides from Erwinia *spp.*—The structures of the *Erwinia* polysaccharides determined to date fall into four families and are presented below.

Family 1, SR 260 Family.

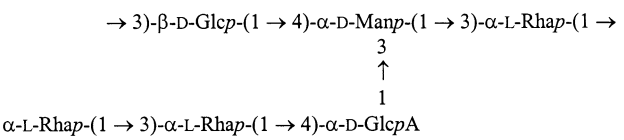

Included in this family are EPSs produced by *E. chrysanthemi* strains Ech1, Ech9, SR31 and Ech378.

Family 2, Ech6 Family.

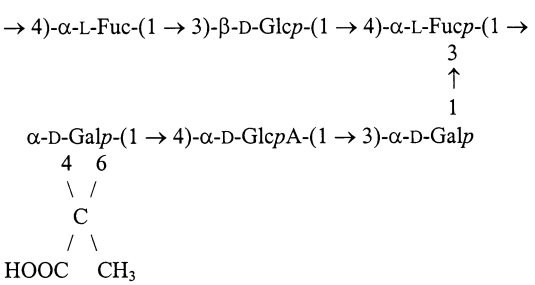

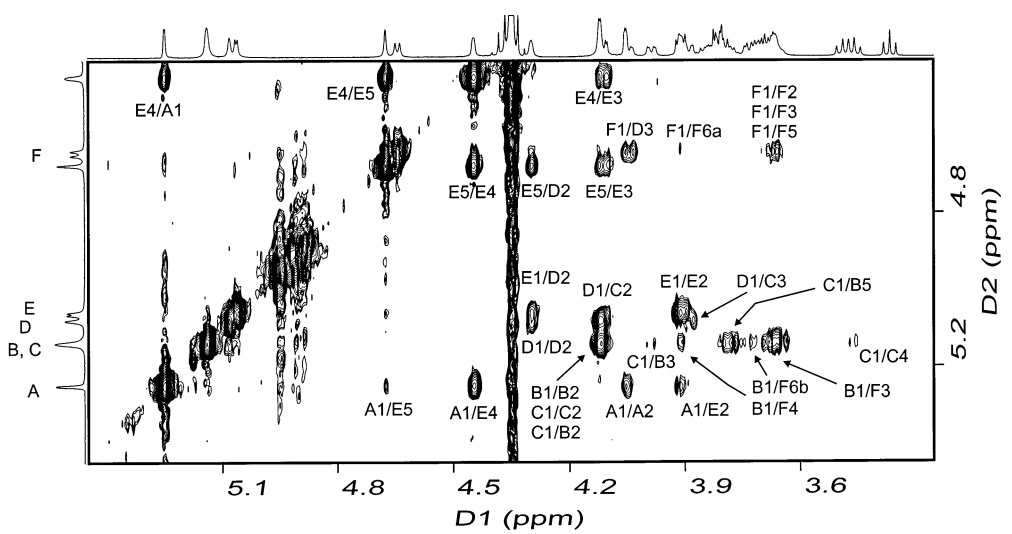

Fig. 6. 2D NOESY spectrum of A350 EPS acquired at 338 K and 600.14 MHz. The mixing time was 150 ms. Both intra- and inter-residue cross-peaks are identified and labeled.

Family 3, CU643 Family.

→3)-β-D-Gal*p*-(1→2)-α-L-Rha*p*-(1→4)-
β-D-Glc*p*A-(1→2)-α-L-Rha*p*-(1→2)-
α-L-Rha*p*-(1→2)-α-Rha*p*-(1→

This is the sole member of this family thus far.

Family 4, A350 Family.

→2)-α-L-Rha*p*-(1→3)-β-D-Gal*p*-(1→3)-α-L-Rha*p*-(1→2)-α-L-Rha*p*-(1→
2
↑
1
α-L-Rha*p*-(1→4)-α-D-Gal*p*A

Preliminary work indicates that the structure of the EPS from A2148 is similar to that from A350 and thus also belongs to this family.

The structure of the EPS from strain A350 is different from those produced by *E. chrysanthemi* strains SR260 [7,8], Ech6 [10], Ech1 and Ech9 [11], all of which contain GlcA rather than GalA. The composition of A350 EPS is similar to that from strain CU643 [9] except that a GalA residue in A350 EPS is present in place of a GlcA residue in CU643 EPS. A major difference between the EPSs from strains A350 and CU643 is that the former is a branched polysaccharide (and is therefore similar to the polysaccharides from other *Erwinia* strains), whereas the latter is unique amongst the *Erwinia* EPSs thus far studied in being a linear molecule [9].

Ribotyping.—All of the strains studied in this laboratory were subjected to biochemical tests in the clinical laboratory and were classified as *Enterobacter* spp. (most commonly *Enterobacter agglomerans*), the clinical equivalent of the *Erwinia* spp. The strains were all pectolytic except for Ech6.

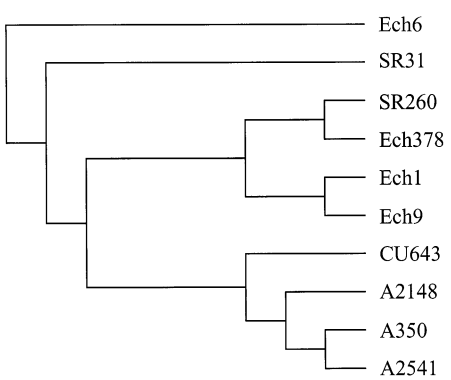

Fig. 7. Nearest-neighbor analysis of the ribotyping data from the *E. chrysanthemi* strains used in this study.

These analyses were not specific enough to differentiate clearly between the different *E. chrysanthemi* spp. being studied. Another means of differentiating the strains was therefore sought. Ribotyping, whereby the relative positions of the ribosomal 16S genes on the chromosome are determined, clearly showed that SR260, Ech1 and Ech9 were not the same species but do share a common branch in the dendrogram (generated by the program NEIGHBOR from the Phylip 3.73c suite of phylogeny programs [29]) (Fig. 7). Intriguingly, strain Ech378 is closely related to SR260, whereas SR31 is not. Significantly, A2148 and A350 are not identical although they are closely related and share a common branch on the dendrogram with strain CU643. As mentioned above, the polysaccharides from strains A350 and A2148 and from strain CU643 share many similarities in their composition, linkages and so on and this similarity is reflected in the ribotyping data.

From the ribotyping data, it was concluded that SR260, Ech1 and Ech9 are indeed different strains that produce an EPS with a common structure. Furthermore, the fact that they are not all pathogenic on the same host suggests that the structure of their extracellular polysaccharide is not a major factor in determining host specificity.

It will be of interest to see if the general structural types of the unstudied EPS predicted by the ribotyping hold true.

Acknowledgements

The authors thank the Biotechnology Byproducts Consortium (USDA Grant No. 94-34188-0039) and the Carbohydrate Structure Facility for the use of its equipment. We also thank John Snyder for recording the ^{1}H NMR spectra and for many discussions, Richard J. Hollis for the ribotyping, and Carol Yang for the clinical microbiological characterizations.

References

[1] F. Barras, F. van Gijsegem, A.K. Chatterjee, *Annu. Rev. Phytopathol.*, 32 (1994) 201–234.

[2] A.K. Chatterjee, M.P. Starr, *Annu. Rev. Microbiol.*, 34 (1980) 645–676.
[3] R.S. Dickey, *Phytopathology*, 69 (1979) 324–329.
[4] R.S. Dickey, *Phytopathology*, 71 (1981) 23–29.
[5] R.S. Dickey, C.H. Zumoff, J.K. Uyemoto, *Phytopathology*, 74 (1984) 1388–1394.
[6] R.S. Dickey, L.E. Claflin, C.H. Zumoff, *Phytopathology*, 77 (1987) 426–430.
[7] J.S.S. Gray, J.M. Brand, T.A.W. Koerner, R. Montgomery, *Carbohydr. Res.*, 245 (1993) 271–287.
[8] J.S.S. Gray, T.A. Koerner, R. Montgomery, *Carbohydr. Res.*, 266 (1995) 153–159.
[9] B.Y. Yang, J.S.S. Gray, R. Montgomery, *Carbohydr. Res.*, 316 (1999) 138–154.
[10] B.Y. Yang, J.S.S. Gray, R. Montgomery, *Int. J. Biol. Macromol.*, 16 (1994) 306–312.
[11] B.Y. Yang, J.S.S. Gray, R. Montgomery, *Int. J. Biol. Macromol.*, 19 (1996) 223–226.
[12] B.Y. Yang, J.S.S. Gray, R. Montgomery, *Carbohydr. Res.*, 296 (1996) 183–201.
[13] P.-E. Jansson, G. Widmalm, *Carbohydr. Res.*, 231 (1992) 325–328.
[14] J.M. Lau, M. McNeil, A.G. Darvill, P. Albersheim, *Carbohydr. Res.*, 168 (1987) 245–274.
[15] J.M. Lau, M. McNeil, A.G. Darvill, P. Albersheim, *Carbohydr. Res.*, 168 (1987) 219–243.
[16] G.J. Gerwig, J.P. Kamerling, J.F.G. Vliegenthart, *Carbohydr. Res.*, 62 (1978) 349–357.
[17] B. Domon, C.E. Costello, *Glycoconjugate J.*, 5 (1988) 397–409.
[18] I.J. Colquhoun, R.G.A. De, H.A. Schols, A.G.J. Voragen, *Carbohydr. Res.*, 206 (1990) 131–144.
[19] H.A. Schols, A.G.J. Voragen, I.J. Colquhoun, *Carbohydr. Res.*, 256 (1994) 97–111.
[20] S.B. Tjan, A.G.J. Voragen, W. Pilnik, *Carbohydr. Res.*, 34 (1974) 15–23.
[21] D.F. Zhan, P. Janssen, A.J. Mort, *Carbohydr. Res.*, 308 (1998) 373–380.
[22] P.-E. Jansson, L. Kenne, H. Ottosson, *J. Chem. Soc., Perkin Trans.*, 1 (1990) 2011–2018.
[23] K. Bock, C. Pedersen, H. Pedersen, *Adv. Carbohydr. Chem. Biochem.*, 42 (1984) 193–225.
[24] I. Tvaroska, F.R. Taravel, *Adv. Carbohydr. Chem. Biochem.*, 51 (1995) 15–61.
[25] P.-E. Jansson, L. Kenne, K. Persson, G. Widmalm, *J. Chem. Soc., Perkin Trans. 1*, (1990) 591–598.
[26] P.-E. Jansson, J. Lindberg, K.M.S. Wimalasiri, M.A. Dankert, *Carbohydr. Res.*, 245 (1993) 303–310.
[27] G. Widmalm, R.A. Byrd, W. Egan, *Carbohydr. Res.*, 229 (1992) 195–211.
[28] V.K. Dua, B.N.N. Rao, S.-S. Wu, V.E. Dube, C.A. Bush, *J. Biol. Chem.*, 261 (1986) 1599–1608.
[29] J. Felsenstein, Phylip (phylogeny inference package), 3.73c (1998), Department of Genetics, University of Washington, Seattle (http://evolution.genetics.washington.edu/phylip.html).